Reports

# Age of Canada Basin Deep Waters: A Way to Estimate Primary Production for the Arctic Ocean

R. W. MACDONALD AND E. C. CARMACK

**An empirical model of carbon flux and $^{14}C$-derived ages of the water in the Canada Basin of the Arctic Ocean as a function of depth was used to estimate the long-term rate of primary production within this region. An estimate can be made because the deep waters of the Canadian Basin are isolated from the world oceans by the Lomonosov Ridge (sill depth about 1500 meters). Below the sill, the age of the water correlates with increased nutrients and oxygen utilization and thus provides a way to model the average flux of organic material into the deep basin over a long time period. The $^{14}C$ ages of the deep water in the Canada Basin were about 1000 years, the carbon flux across the 1500-meter isobath was 0.3 gram of carbon per square meter per year, and the total production was 9 to 14 grams of carbon per square meter per year. Such estimates provide a baseline for understanding the role of the Arctic Ocean in global carbon cycling.**

HIGH-LATITUDE OCEANS ARE ECOlogically sensitive regions where impacts of climate change are believed to be largest and where early detection of change is possible. An obvious consequence of warming in the Arctic Ocean is a change in ice cover and in the structure of the water mass, which would also affect primary production. The present primary production is, however, poorly known. To address the question of how production and change are linked, it is useful to consider total production as composed of new production that results from nutrient transport into the photic zone and regenerated production that results from nutrient recycling in the photic zone (*1, 2*). New production determines the rate at which biologically fixed C can be exported downward from the surface layers of the ocean. For this reason, sediment traps have become the principal tool with which to measure vertical C flux and, by extension, new production (*3*).

The Arctic Ocean is roughly divided at a depth of 1500 m into the Canadian and Eurasian basins by the Lomonosov Ridge (Fig. 1); the Canadian Basin is further divided into the Canada and Makarov basins by the Alpha-Mendeleyev Ridge. A deep ocean basin with restricted circulation, such as the Canada Basin, is analogous to a sediment trap in that it, too, captures sinking particles and therefore records the influx of sinking, particulate organic C. In this report, we pursue this analogy by developing a mixing model for the $^{14}C$ age of deep water. We use this model to compute $O_2$ utilization and nutrient regeneration rates for the basin and then calculate the C flux below 1500 m. Finally we relate this C flux to total production using available empirical models.

The Canada Basin is an ideal site for examining the relation between water mass history and rates of change of C, $O_2$, and nutrient inventories. Its deep waters are isolated from the world ocean and are old (*4*); furthermore, the temperature profile below sill depth is adiabatic, and salinities are slightly higher than for water east of the Lomonosov Ridge (*5, 6*). The conventional view on the origin of the deep water is that it is derived from the Norwegian Sea by flow through the Fram Strait and over the ridge (*7, 8*). This hypothesis accounts for temperature distribution but not the high salinity. Aagaard *et al.* (*9*) proposed that some excess salt may come from the surrounding continental shelves where salinity is increased by freezing at the surface. However, this notion is supported neither by recent $\delta^{18}O$ and tritium measurements (7) (Table 1) nor by nutrient ratio tracers (*10*), both of which imply that shelf-derived water contributes less than 10 to 15% of the water in the basin. Alternatively, the excess salt may, like the $^{14}C$, be relict and derive from an earlier, more saline Arctic Ocean and Greenland Sea (*11*). If, for example, the Greenland Sea produced deep water that was 0.04 more saline than today a millennium ago, then subsequent freshening of the source water would stop active ventilation of the Canadian Basin. This high salinity of the Canadian Basin underscores the main difference between the deep water of the Eurasian Basin, which is modern, and that of the Canadian Basin, which is relict. We thus suggest that the Canada Basin can be treated as a long-term repository of regenerated organic material.

We sampled the deep waters of the southern Canada Basin during a cruise aboard the C.C.G.S. *Sir John Franklin* in September 1989 (Fig. 1). Water samples were collected with 5-liter Niskin bottles; $NO_3^-$ and $O_2$ were determined within 24 hours of sampling. Standard methods were used to de-

**Fig. 1.** Bathymetric map of the Arctic Ocean and the location of station A1 in the southern Canada Basin.

---

Institute of Ocean Sciences, Post Office Box 6000, Sidney, British Columbia, Canada V8L 4B2.

termine $NO_3^-$, dissolved $O_2$, salinity, and temperature (*12*). The $^{14}C$ measurements were performed on 1-liter water samples by accelerator mass spectrometry at the University of Toronto (IsoTrace Radiocarbon Laboratory); the results (Table 1) are the average of four machine-ready targets (high precision) and have been corrected for natural and sputtering fractionation. Conventional radiocarbon ages were calculated with the use of the Libby $^{14}C$ mean life of 8033 years and have been fractionation-corrected to a base of $\delta^{13}C = -25$ per mil (*13*).

**Table 1.** Data collected (only data for >1000 m are given) at station A1, 72°34.0′N, 143°25.6′W. $T$ is potential temperature. Age is in years BP (1989). Pooled standard deviations ($s_p$) for duplicate measurements are as follows: temperature, 0.024; salinity, 0.01; $O_2$, 0.65; $NO_3^-$, 0.08. For the $^{14}C$ measurements, the errors are $1\sigma$ and include analytical and fractionation corrections. Tritium measurements were provided by G. Ostlund, University of Miami ($1\sigma = 0.09$); $\delta^{18}O$ measurements were done by M. Stuiver, Quaternary Research Laboratory, University of Washington ($1\sigma < 0.07$).

| Depth (m) | $T$ (°C) | Salinity | $O_2$ (mmol $m^{-3}$) | $NO_3^-$ (mmol $m^{-3}$) | TU81N* | $\delta^{18}O$ (per mil) | $\Delta^{14}C$ (per mil) | Age |
|---|---|---|---|---|---|---|---|---|
| 1000 | +0.03 | 34.880 | 309 | 12.9 | 2.59 | 0.32 | | |
| 1250 | −0.24 | 34.899 | 309 | 13.3 | 1.96 | 0.38 | −7 ± 6 | 60 ± 50 |
| 1500 | −0.38 | 34.915 | 309 | 13.6 | 2.15 | 0.40 | −29 ± 5 | 240 ± 40 |
| 1600 | −0.47 | 34.913 | 306 | 13.8 | 1.15 | 0.42 | | |
| 1700 | −0.47 | 34.919 | 305 | 14.1 | | | | |
| 1800 | −0.50 | 34.924 | 305 | 14.1 | | | −62 ± 6 | 510 ± 50 |
| 1900 | −0.45 | 34.926 | 302 | 14.3 | | | | |
| 2000 | −0.53 | 34.930 | 302 | 14.4 | 0.31 | 0.43 | −64 ± 6 | 530 ± 50 |
| 2250 | −0.55 | 34.939 | 298 | 14.7 | 0.16 | 0.49 | −82 ± 6 | 690 ± 50 |
| 2500 | −0.52 | 34.940 | 296 | 14.8 | 0.00 | 0.41 | −104 ± 7 | 880 ± 60 |
| 3000 | −0.51 | 34.946 | 294 | 14.8 | −0.21 | 0.42 | −105 ± 6 | 890 ± 50 |
| 3100 | −0.52 | 34.953 | 292 | 14.8 | −0.08 | 0.44 | −118 ± 17 | 1010 ± 160 |
| 3200 | −0.52 | 34.940 | 294 | 14.8 | 0.14 | 0.47 | | |

*Tritium assays are expressed in the ratio T/H × $10^{-18}$; this TU value is corrected for radioactive decay by referencing it to 1 January 1981, using a half-life of 12.43 years.

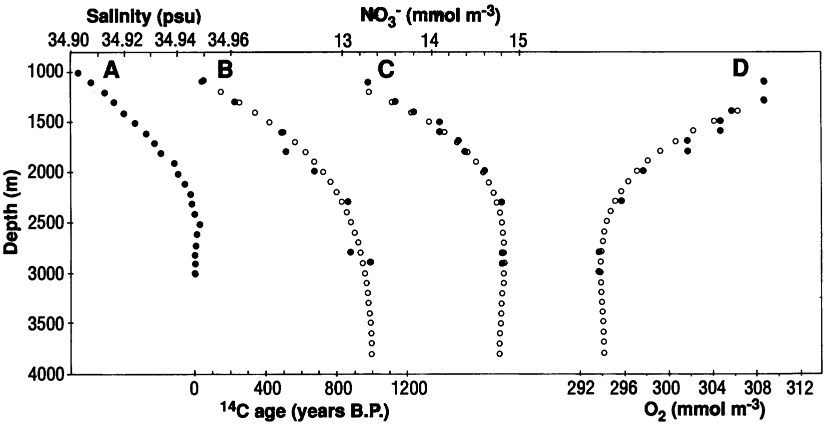

**Fig. 2.** Vertical profiles of (**A**) salinity (psu = practical salinity unit), (**B**) $^{14}C$ age, (**C**) $NO_3^-$ concentration, and (**D**) dissolved $O_2$ concentration. Solid circles denote measurements, open circles show the model results for geochemical properties.

The data record a relatively steady increase in salinity between 1500 and 2000 m, the level of the Lomonosov Ridge, and a near-adiabatic potential temperature profile below this depth (Fig. 2A). Dissolved $O_2$ decreased and nutrients increased monotonically toward the bottom. The apparent $^{14}C$ age increased from 60 years at 1500 m to 1010 years in the deepest sample at 3100 m. Accompanying samples measured for tritium and $\delta^{18}O$ showed no evidence of modern inputs.

The above data lead us to suppose that the deep waters are indeed relict; other data also show that lateral gradients are small (*14*); thus the system can be modeled as a one-dimensional, time-dependent, diffusive system with appropriate rate and decay functions (*15*). Specifically, for $^{14}C$

$$\frac{\partial^{14}C}{\partial t} = K_z \frac{\partial^2\,{}^{14}C}{\partial z^2} - \lambda^{14}C \qquad (1)$$

where $K_z$ is the vertical diffusion coefficient, and $\lambda$ is the decay constant for $^{14}C$ (8033 $year^{-1}$). To integrate this equation, we must assume that at some time in the past the salinity (density) within the Eurasian Basin at sill depth decreased by some small fraction sufficient to stop ventilation of the Canadian Basin while at the same time other scalar water properties remained constant at the sill depth. This integration has been carried out numerically (*16*) for a range of $K_z$ values to match the observed $^{14}C$ ages; the best fit occurs with $K_z = 2.3 \times 10^{-5}\ m^2\ s^{-1}$ and an integration time of 983 years (Fig. 2B). These values for $K_z$ and time can now be used to constrain the conservation equations for $O_2$ and $NO_3^-$:

$$\frac{\partial X_i}{\partial t} = K_z \frac{\partial^2 X_i}{\partial z^2} + R_i \qquad (2)$$

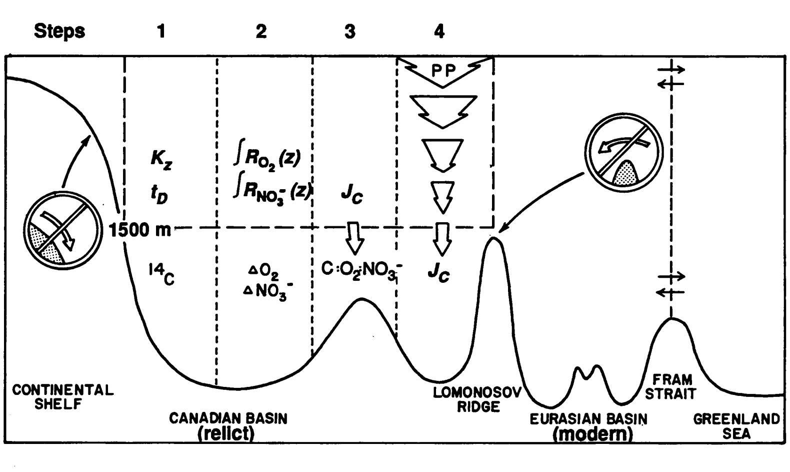

**Fig. 3.** Scheme showing an idealized section across the Arctic Ocean from the Canadian continental shelf to the Greenland Sea and illustrating the construction of the model used in this paper. We assumed that there was no deep ventilation below 1500 m in the Canada Basin from either the continental shelf or the Eurasian Basin. In step 1, the vertical diffusion coefficient $K_z$ and integration time $t_D$ were varied to obtain the best fit for the $^{14}C$ profile. In step 2, we assumed that the observed changes in $O_2$ and $NO_3^-$ were driven by the integrated fallout and regeneration of organic material from new production. In step 3, stoichiometric ratios were used to calculate the flux of organic material into deep water of the basin averaged over the time period $t_D$. In step 4, the flux of organic material across the 1500-m boundary was related to new production through an empirical model.

where $X_i$ is the concentration of some biogenic, nonconservative property and $R_i$ is its regeneration rate. In order to formulate $R_i$, an assumption must be made concerning its depth dependence; following Suess (*17*), we set $R_i = kz_i^{-1}$ and varied $k$ to achieve the best fit to the data (Fig. 2, C and D). This value of $k$ was then used to find the material flux, $J$, across the 1500-m boundary that is required to support the changes in biogenic properties below the sill depth. This relation is integrated to the bottom. The calculated $NO_3^-$ flux is 3.2 mmol $m^{-2}$ $year^{-1}$, and the $O_2$ utilization rate is 32 mmol $m^{-2}$ $year^{-1}$. The flux of $NO_3^-$ or $O_2$ can then be related to C flux, $J_C$, through the Redfield stoichiometric relation: $\Delta N:\Delta O_2:\Delta C = 16:-138:106$. This approach gives two estimates for $J_C$: one based on $O_2$ consumption (0.30 g C $m^{-2}$ $year^{-1}$) and one based on $NO_3^-$ regeneration (0.26 g C $m^{-2}$ $year^{-1}$). Finally, the total capture of C, integrated over the basin area ($5.7 \times 10^6$ $km^2$), is $1.7 \times 10^{12}$ g C $year^{-1}$.

Total production (PP) can be computed by application of an appropriate model to the C flux across the 1500-m boundary (Fig. 3). From the selection of models offered by Bishop (*3*) we have chosen those of Suess (*17*) [$J = PP/(0.024z + 0.21)$] and Berger *et al.* (*18*) ($J = 17\ PP/z + PP/100$), the latter of which is probably more appropriate to the deep water column. These models yield values of total PP ranging from 9 to 14 g C $m^{-2}$ $year^{-1}$. If one uses the relation proposed by Berger *et al.* (*19*) to estimate new production ($NP = PP^2/410$), NP is about 0.5 g C $m^{-2}$ $year^{-1}$.

It is difficult to measure PP in the Arctic Ocean directly because ice cover limits ship access and blankets coverage by remote sensing. Earlier estimates (mostly from shelves) have been based on $^{14}C$ uptake (*20, 21*), nutrient budgets (*22*), time-dependent chemical tracers (*23*), and the $CO_2$ system (*24*); they range from 1 to 45 g C $m^{-2}$ $year^{-1}$. Our estimate, based on treating the system as a time-dependent, nutrient-regenerating water mass falls at the low end of this range; it represents a millennium-long average, well suited as a backdrop for comparison of shorter term fluctuations. It must be considered a minimum, however, because we have ignored in the calculation material that becomes permanently preserved in the sediment, a fraction generally presumed to be small. For example, Berger *et al.* (*18, 19*) suggested that most of the organic C arriving at the sea floor is consumed near the interface; perhaps only 10% of what reaches the deep ocean sediments is permanently preserved. Although the empirical models used here were developed in temperate oceans, data from the Antarctic suggest they may also be used in ice-covered seas (*25*). Clearly, to verify this approach, we need to develop better models of particle flux and C regeneration applied specifically to polar environments on the basis of time series data from sequential sediment traps. Other questions remain: what controls the resupply of $NO_3^-$ to surface water, and how much of the deep C flux derives from shelf and slope regions?

---

### REFERENCES AND NOTES

1. R. C. Dugdale and J. J. Goering, *Limnol. Oceanogr.* **23**, 196 (1967).
2. R. W. Epply and B. J. Peterson, *Nature* **282**, 677 (1979).
3. J. K. B. Bishop, in *Productivity of the Ocean: Past and Present*, W. H. Berger, V. S. Smetacek, G. Wefer, Eds. (Wiley, Chichester, 1989), pp. 117–137.
4. H. G. Ostlund, G. Possnert, J. H. Swift, *J. Geophys. Res.* **92**, 3769 (1987).
5. K. Aagaard, *Deep-Sea Res.* **28**, 251 (1981).
6. J. H. Swift and K. P. Koltermann [*J. Geophys. Res.* **93**, 3563 (1988)] discussed salinity variability within the deep waters of the Arctic-Mediterranean system.
7. E. C. Carmack, in *Polar Oceanography*, part A, *Physical Science*, W. O. Smith, Ed. (Academic Press, San Diego, 1990), pp. 171–222; $\delta^{18}O = [(^{18}O/^{16}O_{sample} - ^{18}O/^{8}O_{SMOW})/(^{18}O/^{16}O_{SMOW})] \cdot 10^3$, where SMOW is standard mean ocean water.
8. W. G. Metcalf, *Deep-Sea Res.* 7, 190 (1960).
9. K. Aagaard, J. H. Swift, E. C. Carmack, *J. Geophys. Res.* **90**, 4833 (1985).
10. C. Wilson and D. W. R. Wallace, *ibid.* **95**, 22193 (1990).
11. F. Bryan [*Nature* **323**, 301 (1986)] introduced the notion that long-term fluctuations in deep-water salinity can influence the thermohaline circulation.
12. R. W. Macdonald *et al.*, *Can. Data Rep. Hydrogr. Ocean Sci.* 80 (1990).
13. R. P. Beukens, D. M. Gurfinkel, H. W. Lee, *Radiocarbon* **28**, 229 (1986).
14. The deep water (<1250 m) in the Canada Basin was also sampled at T3 [P. Kinney *et al.*, *J. Geophys. Res.* **75**, 4097 (1973)], LOREX [R. M. Moore *et al.*, *ibid.* **88**, 2667 (1983)], and AIWEX (J. H. Swift, personal communication).
15. M. Scranton *et al.*, *Deep-Sea Res.* **34**, 945 (1987).
16. The model used here follows that of Scranton *et al.* (*15*). Integrations were carried out over the depth range of 1400 to 4000 m with 100-m depth intervals, and time steps of 1 year. Initial conditions were chosen from present-day values at sill depth; for example $^{14}C$ age = 60 years, $NO_3^-$ = 13.3 mmol $m^{-3}$, and $O_2$ = 309 mmol $m^{-3}$. We applied hypsographic corrections, using Aagaard *et al.* (*9*).
17. E. Suess, *Nature* **288**, 260 (1980).
18. W. H. Berger *et al.*, in *Biogeochemical Cycling and Fluxes Between the Deep Euphotic Zone and Other Oceanic Realms*, C. Agegian, Ed. (National Oceanic and Atmospheric Administration Symposium Series for Undersea Research, U.S. Department of Commerce, Washington, DC, 1987), pp. 131–176.
19. W. H. Berger, V. S. Smetacek, G. Wefer, in *Productivity of the Ocean: Past and Present*, W. H. Berger, V. S. Smetacek, G. Wefer, Eds. (Wiley, Chichester, 1989), pp. 1–34.
20. D. V. Subba-Rao and T. Platt, *Polar Biol.* **3**, 191 (1984).
21. T. S. English, *Arctic Inst. North Am. Res. Pap.* 13 (1961).
22. R. W. Macdonald, C. S. Wong, P. Erickson, *J. Geophys. Res.* **92**, 2939 (1987).
23. D. W. R. Wallace, R. M. Moore, E. P. Jones, *Deep-Sea Res.* **34**, 1957 (1987).
24. L. Anderson, D. Dyrssen, E. P. Jones, *J. Geophys. Res.* **95**, 1703 (1990).
25. G. Wefer, G. Fischer, D. Fuetterer, R. Gersonde, *Deep-Sea Res.* **35**, 891 (1988).
26. We thank E. P. Jones, K. Aagaard, and two anonymous reviewers for helpful comments. In particular, we thank Captain D. Johns and I. Cote of Coast Guard Northern for their continuing efforts to provide oceanographic platforms, and Captain D. S. McGarvie, the officers, and crew of C.C.G.S. *Sir John Franklin*. Nutrient and $O_2$ determinations were provided by F. McLaughlin and M. O'Brien. This work was jointly supported by Fisheries and Oceans Canada and Indian and Northern Affairs Canada under Northern Oil and Gas Action Program B.6.

6 June 1991; accepted 13 August 1991

---

# Orientational Disorder in Solvent-Free Solid $C_{70}$

Gavin B. M. Vaughan, Paul A. Heiney,* John E. Fischer,
David E. Luzzi, Deborah A. Ricketts-Foot, Andrew R. McGhie,
Yiu-Wing Hui, Allan L. Smith, David E. Cox,
William J. Romanow, Brent H. Allen, Nicole Coustel,
John P. McCauley, Jr., Amos B. Smith III

**The high-temperature structure of solvent-free $C_{70}$ has been determined with high-resolution x-ray powder diffraction and electron microscopy. Samples crystallized from solution form hexagonal close-packed crystals that retain an appreciable amount of residual toluene, even after prolonged heating. Samples prepared by sublimation, which contain no detectable solvent, are primarily face-centered cubic with some admixture of a hexagonal phase. The relative volume of the hexagonal phase can be further reduced by annealing. The structures of both phases are described by a model of complete orientational disorder. The cubic phase contains an appreciable density of stacking faults along the [111] direction.**

SOLID $C_{60}$ IS A VAN DER WAALS-bonded molecular crystal (*1*) which exhibits an orientational ordering transition at $T_c = 249$ K (*2*). Both high- and low-temperature structures are characteristic of cubic close-packed pseudospheres, consistent with the molecular geometry (*3*). At high temperature ($T$), all molecules are crystallographically equivalent due to dynamic orientational disorder (*4*), while at low temperature the dynamics are frozen out to yield a simple cubic structure with *Pa3* symmetry, thus breaking the orientational equivalence (*2, 5–8*). The next-larger fullerene, $C_{70}$, is of lower $D_{5h}$ symmetry (*9*) (Fig. 1, inset). Its elongated "rugby-ball" shape should inhibit free rotations, thus increasing $T_c$. The reduced sym-